Precambrian Research 167 (2008) 267–280

Contents lists available at ScienceDirect

Precambrian Research

journal homepage: www.elsevier.com/locate/precamres

Palaeomagnetism of red beds from the Kimberley Group, Western Australia: Implications for the palaeogeography of the 1.8 Ga King Leopold glaciation

Phillip W. Schmidt [a,*], George E. Williams [b]

[a] CSIRO Exploration and Mining, PO Box 136, North Ryde, NSW 1670, Australia
[b] Discipline of Geology and Geophysics, School of Earth and Environmental Sciences, University of Adelaide, SA 5005, Australia

ARTICLE INFO

Article history:
Received 1 May 2008
Received in revised form 11 August 2008
Accepted 1 September 2008

Keywords:
Palaeoproterozoic
Elgee Siltstone
Pentecost Sandstone
Lansdowne Arkose
Hematite
Regolith

ABSTRACT

The 1.8 Ga King Leopold glaciation in northwestern Australia is recorded in the Kimberley Basin by subglacial erosional forms cut in an unconformity surface at the top of the Speewah Group and buried by glaciofluvial deposits at the base of the King Leopold Sandstone, the lowest formation of the Kimberley Group. The glaciofluvial deposits are conformably overlain by texturally mature, locally glauconitic quartzarenite of shallow-marine origin, implying that glaciation occurred near sea level. Palaeomagnetic data for five sites (29 specimens) in the hematite-bearing Elgee Siltstone of the upper Kimberley Group in the northeastern Kimberley Basin gave a dip-corrected mean direction of declination $D = 95.4^\circ$, inclination $I = 13.8^\circ$ ($\alpha_{95} = 9.7^\circ$), indicating a palaeolatitude $\lambda = 7.0\ +5.3/-5.0^\circ$. Results for red beds from five sites (28 specimens) in the conformably overlying Pentecost Sandstone gave a dip-corrected mean direction of $D = 94.1^\circ$, $I = 13.0^\circ$ ($\alpha_{95} = 11.7^\circ$), $\lambda = 6.6\ +6.4/-5.9^\circ$. Combining our data for the Elgee Siltstone and Pentecost Sandstone with results for the Elgee Siltstone in the southeastern Kimberley Basin [Li, Z.X., 2000. Palaeomagnetic evidence for unification of the North and West Australian cratons by *ca.* 1.7 Ga: new results from the Kimberley Basin of northwestern Australia. Geophysical Journal International 142, 173–180.] yielded a dip-corrected mean direction for 17 sites of $D = 93.5^\circ$, $I = 15.1^\circ$ ($\alpha_{95} = 4.4^\circ$), palaeolatitude $\lambda = 7.7 \pm 2.3^\circ$, and an overall pole position at latitude $\lambda_p = 5.4^\circ$S, longitude $\varphi_p = 211.8^\circ$E, with confidence semi-axes $d_p = 2.3^\circ$ and $d_m = 4.5^\circ$. A positive fold test at 99% confidence was obtained for the combined data for the 17 sites. The basinwide concordance of results for the Elgee Siltstone and the positive fold test argue for an early magnetisation acquired prior to late Palaeoproterozoic initial folding of the Kimberley Group and close to the time of deposition. Our results imply a low palaeolatitude for the Kimberley Group and the King Leopold glaciation. Palaeomagnetic data for the 1.822 Ga Plum Tree Creek Volcanics in the Pine Creek Orogen to the east of the Kimberley Basin are consistent with northwestern Australia being in low palaeolatitudes during the late Palaeoproterozoic. Hence the enigma of glaciation near sea level in low palaeolatitudes, which marks the Neoproterozoic and early Palaeoproterozoic, applies also to the late Palaeoproterozoic.

Red beds from the Lansdowne Arkose of the Speewah Group also were studied, but only directions ascribable to Tertiary regolith weathering processes were found. Similar findings for the late Palaeoproterozoic McArthur Basin in northern Australia suggest some units in that basin also record Tertiary regolith processes.

1. Introduction

Palaeoclimatologists have long thought that a global non-glacial interval occurred from 2200 to 800 Ma between the early Palaeoproterozoic and late Neoproterozoic glaciations recognised on most continents (Crowell, 1999), and a strong atmospheric greenhouse effect was postulated for that interval (Pavlov et al., 2003). The Kimberley region in Western Australia (Fig. 1), however, contains evidence of a late Palaeoproterozoic (~1800 Ma) glacial event, called the "King Leopold glaciation" (Williams, 2004, 2005), that punctuates this putative Proterozoic non-glacial interval.

Sparse palaeomagnetic data for late Palaeoproterozoic rocks in the Kimberley region (McElhinny and Evans, 1976; Li, 2000) suggested a low palaeolatitude (<20°) for the King Leopold glaciation, comparable with the low palaeolatitudes determined for other Proterozoic glaciations (e.g. Schmidt and Williams, 1995; Park, 1997; Evans et al., 1997; Williams and Schmidt, 1997, 2004; Evans, 2000). Here we present new palaeomagnetic data for late Palaeoproterozoic sedimentary rocks from the Kimberley region that bear on the palaeogeography and palaeolatitude of the King Leopold

* Corresponding author. Fax: +61 2 9490 8874.
E-mail address: phil.schmidt@csiro.au (P.W. Schmidt).

0301-9268/$ – see front matter.
doi:10.1016/j.precamres.2008.09.002

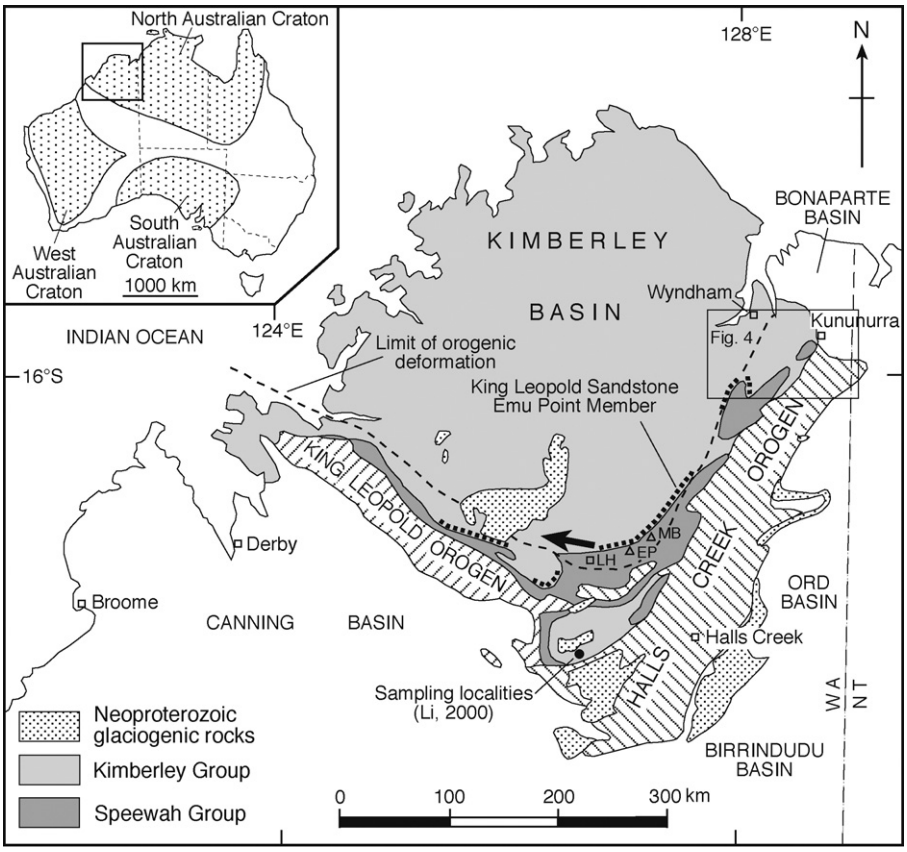

Fig. 1. Extent of the late Palaeoproterozoic Kimberley Group in the Kimberley Basin, the late Palaeoproterozoic Speewah Group, Neoproterozoic sedimentary rocks, and the King Leopold and Halls Creek orogens, Western Australia. The bold dotted line marks the simplified line of outcrop of the glaciofluvial Emu Point Member at the base of the 1.8 Ga King Leopold Sandstone, and the arrow indicates the direction of ice flow for the King Leopold glaciation. Box on the right shows the area of sampling sites for the Kimberley Group in the present study (Fig. 4). LH, Lansdowne homestead; EP, Emu Point; MB; Mount Bedford. Modified after Williams (2005). Inset shows the main Precambrian cratons of Australia (modified after Myers et al., 1996).

glaciation. Our findings are relevant to the current debate concerning Proterozoic glacial environments (e.g. Jenkins et al., 2004).

2. Geological setting

The Kimberley region in northwestern Australia contains up to 7 km of late Palaeoproterozoic siliciclastic and carbonate sedimentary rocks and basalt of the Speewah and Kimberley groups that unconformably overlie late Palaeoproterozoic basement complexes. The stratigraphy and available geochronological data are summarised in Fig. 2. The Kimberley Group (Table 1) in the Kimberley Basin covers most of the region and is envisaged to have accumulated in a broad, semi-enclosed shallow-marine basin (Plumb et al., 1990). The Kimberley Group is unmetamorphosed and is essentially undeformed except where it is upturned and faulted along the southeastern and southwestern margins of the Kimberley Basin. The unconformably underlying Speewah Group in the Speewah Basin is exposed only in the southeast and southwest (Griffin and Grey, 1990).

A regionally extensive, very low-angle ($\leq 2^\circ$) unconformity to disconformity occurs between the Bedford Sandstone at the top of the Speewah Group and the King Leopold Sandstone at the base of the Kimberley Group (Williams, 1969, 2004, 2005; Griffin et al., 1993; Sheppard et al., 1997; Thorne et al., 1999). The basin-wide, dominantly quartzarenite succession of the King Leopold Sandstone (Table 1) contains scattered grains of glauconite and is interpreted to have been deposited in a shallow epeiric sea marked by strong subtidal currents and local exposure and desiccation of mud flats (Gellatly et al., 1970; Williams, 2005). Tholeiitic basalts of the Carson Volcanics overlie the King Leopold Sandstone (Gellatly et al., 1975). The Hart Dolerite intrudes principally the Speewah Group and lower Kimberley Group, with thin sills intruding units as young as the Pentecost Sandstone (Gellatly et al., 1975; Griffin et al., 1993). The Kimberley Group is unconformably overlain by the late Palaeoproterozoic Bastion Group in the northeast (Thorne et al., 1999) and by Neoproterozoic strata including glaciogenic deposits in the south and southeast (Griffin and Grey, 1990).

A maximum age for the Kimberley Group is provided by a U–Pb zircon age of 1834 ± 3 Ma for felsic volcanic rocks from the Valentine Siltstone of the Speewah Group (Page and Sun, 1994). A minimum age for the Kimberley Group is given by a U–Pb zircon age of 1790 ± 4 Ma for the Hart Dolerite (Ozchron, 2004). The youngest detrital zircon from the Warton Sandstone gave a U–Pb age of 1786 ± 14 Ma (McNaughton et al., 1999). Diagenetic xenotime ages of 1704 ± 7 and 1704 ± 14 Ma were obtained for the Warton Sandstone and Pentecost Sandstone, respectively (McNaughton et al., 1999).

3. King Leopold glaciation

The Bedford Sandstone in the southeastern Kimberley Basin between Lansdowne homestead and Mount Bedford comprises medium- to very coarse-grained, cross-bedded, feldspathic sandstone. A gently dipping (5–15°), near-planar unconformity surface

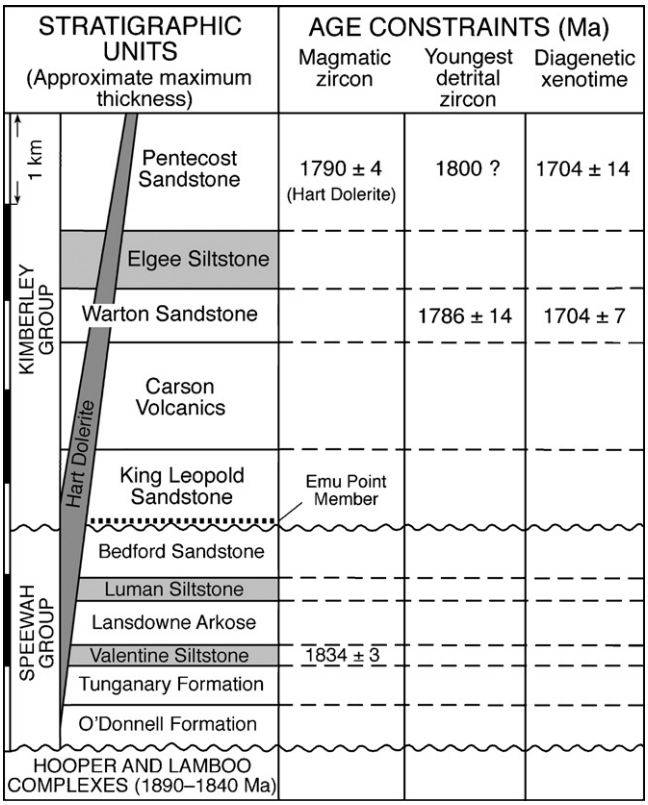

Fig. 2. Generalised stratigraphic column for the Kimberley and Speewah groups, with published U–Pb ages (in Ma). Modified after McNaughton et al. (1999) and Williams (2005). The age of the Hooper and Lamboo basement complexes in the King Leopold and Halls Creek orogens is from Griffin et al. (1993) and Thorne et al. (1999). Formations intruded by the Hart Dolerite are from Gellatly et al. (1975) and Griffin et al. (1993).

Table 1
Conformable succession of the late Palaeoproterozoic Kimberley Group and main features of the King Leopold Sandstone, Kimberley Basin, Western Australia (modified after Derrick et al., 1965; Plumb and McGovern, 1968; Plumb and Gemuts, 1976; Williams, 2005).

Pentecost Sandstone (420–1350+ m)
Upper member. Medium-grained quartzose sandstone, rare coarse-grained sandstone at base; ferruginous sandstone and siltstone
Middle member. Fine- to medium-grained, red brown and white quartzose sandstone, red brown siltstone; minor feldspathic sandstone; glauconitic sandstone at base
Lower member. Fine- to medium-grained, red brown and white quartzose sandstone, red brown siltstone, and feldspathic sandstone

Elgee Siltstone (40–480 m)
Red brown siltstone, red brown and white quartzose sandstone, green mudstone
Teronis Member (0–140 m). Dolostone, mudstone, fine-grained sandstone, abundant stromatolites. Locally at base of the Elgee Siltstone

Warton Sandstone (60–600 m)
White quartzose sandstone, and pale purple and brown feldspathic sandstone, minor mudstone. Cross-bedding, ripple marks, clay pellets
Buckland Point Member (550 m). Quartzose and ferruginous sandstone. Locally at top of the Warton Sandstone

Carson Volcanics (60–1140 m)
Tholeiitic basalt, commonly altered to spilite, amygdaloidal in part, local pillow structure; rhyolitic tuff, agglomerate; feldspathic sandstone, siltstone, chert

King Leopold Sandstone (≤840 m)
White, pale pink and pale purple, texturally mature, fine- to coarse-grained quartzarenite, locally glauconitic; local bands of granules and small pebbles; rare shale beds. Trough and tabular cross-bedding; symmetrical, asymmetrical and interference ripple marks; local planar-bedding with primary current lineation; polygonal mudstone intraclasts. Southward directed palaeocurrents. Conformably overlies the Emu Point Member
Emu Point Member (1–15 m). Poorly sorted quartz-pebble and sandstone-boulder conglomerate; medium-grained to granule sandstone. Trough cross-bedding; rare ventifacts and striated clasts. Westward directed palaeocurrents. East–west oriented grooves (Nye channels), sculpted forms and sandstone-filled vertical cracks (frost fissures) locally in the Bedford surface at the top of the Speewah Group, which the Emu Point Member unconformably to disconformably overlies

at the top of the Bedford Sandstone, here termed the *Bedford surface*, is well exposed in this area (Williams, 2004, 2005). Essentially straight, near-parallel, east–west (100–280°) trending grooves (Fig. 3a) up to tens of metres long and associated erosional features, including etched and undercut cross-strata, undercut meandering channels, *sichelwannen*, potholes and residual ridges, are displayed by the Bedford surface over an east–west distance of 1 km to the north of Lansdowne homestead. These features are interpreted as subglacial Nye channels and sculpted forms (Williams, 2004, 2005). Vertical, sandstone-filled cracks up to 5 cm wide in the Bedford surface are interpreted as fossil frost fissures. The channels in the Bedford surface are remarkably similar to grooves in a 100 m × 100 m smooth surface formed on Pennsylvanian sandstone in Indiana, which Gray (2001) interpreted as Nye channels cut by subglacial meltwaters near the distal margin of a Pleistocene continental ice sheet. Gray (2001) suggested that these Pleistocene Nye channels may have been initiated by glacial abrasion of the Pennsylvanian sandstone.

The Bedford surface is unconformably overlain by up to 15 m of poorly sorted pebble conglomerate (Fig. 3b), boulder conglomerate

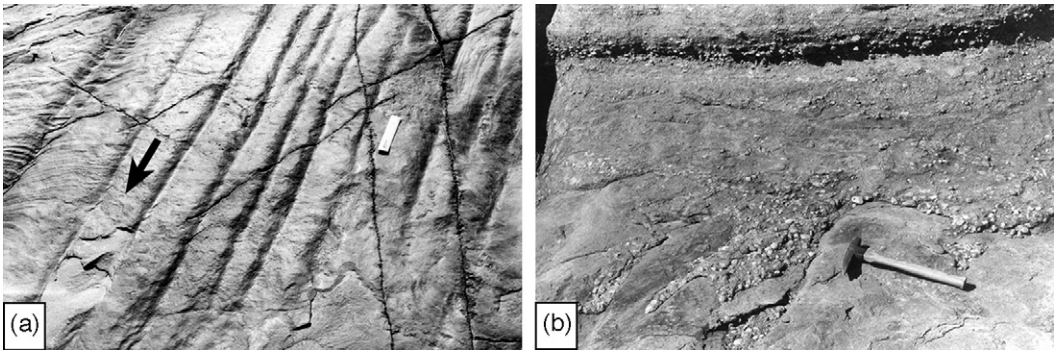

Fig. 3. (a) Nye channels in the Bedford surface developed on the Bedford Sandstone north of Lansdowne homestead. The channels cut across traces of cross-strata in the Bedford Sandstone and are independent of jointing. The arrow shows the palaeocurrent direction for the overlying Emu Point Member and the inferred direction of ice flow. Scale 15 cm. (b) Pebble conglomerate and coarse-grained sandstone of the Emu Point Member unconformably overlying the Bedford surface. Nye channels in the Bedford surface are partly filled with conglomerate, to left of 35 cm hammer.

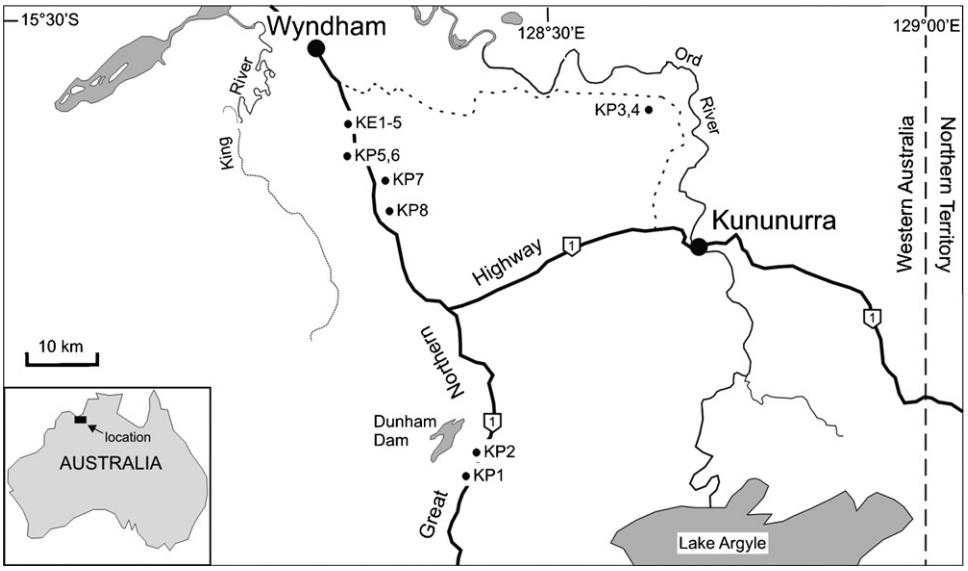

Fig. 4. Map showing palaeomagnetic sampling sites in the Elgee Siltstone (KE) and Pentecost Sandstone (KP) for the present study. Site details are given in Appendix A.

and cross-bedded sandstone at the base of the King Leopold Sandstone (Table 1). This rudaceous facies has a strike length of >300 km and is well developed between Lansdowne homestead and Mount Bedford; it is named here the *Emu Point Member* after a topographic feature where the facies is prominent. The orientation of trough cross-bedding in the sandstone indicates palaeocurrents directed to the west. Ventifacts occur locally in the conglomerates. The Emu Point Member is interpreted as glaciofluvial (Williams, 2004, 2005) and is conformably followed by shallow-marine, texturally mature quartzarenite of the King Leopold Sandstone.

The Bedford surface locally shows relief of 1–10 m where depressions bounded by vertical joints in the Bedford Sandstone are filled by the Emu Point Member. These and other erosional features in the Bedford surface, and the absence of ductile deformation at the top of the Bedford Sandstone, indicate that the Bedford Sandstone was at least moderately lithified prior to the formation of the Nye channels and sculpted forms and deposition of the Emu Point Member. The lithological similarity of the Bedford Sandstone and boulders in the Emu Point Member is consistent with the Bedford Sandstone being lithified prior to its erosion and burial.

A genetic connection between the development of the Nye channels and sculpted forms in the Bedford surface and glaciofluvial deposition is implied by the agreement of the east–west trend of the Nye channels, the westward flow direction of meltwaters indicated by the orientation of sculpted forms, and the westward palaeocurrent direction determined for the overlying glaciofluvial sandstone (Williams, 2005). This agreement of trends and directions is explicable by the westward advance of grounded ice at ~1800 Ma that cut glacial grooves in the moderately lithified Bedford Sandstone, followed soon after by westward-flowing subglacial meltwaters that cut the Nye channels along the original line of the grooves, produced numerous sculpted forms and deposited the Emu Point Member. Glaciation evidently was initiated in the Halls Creek Orogen to the east, with the shallow-marine setting for the bulk of the King Leopold Sandstone implying that grounded ice reached close to sea level. The presence of fossil frost fissures in the Bedford surface indicates that a frigid periglacial climate existed near sea level following glacial retreat, with mean annual air temperatures of <0 to <−4 °C and rapid drops of air temperature between −10 and −20 °C (Williams, 2005).

4. Previous palaeomagnetic studies

Few palaeomagnetic data are available for Palaeoproterozoic rocks in the Kimberley region. McElhinny and Evans (1976) collected three samples at each of 18 sites in the Hart Dolerite in the southeastern Kimberley region. Alternating field (AF) demagnetisation yielded a mean direction of $D = 121°$, $I = 2°$ ($\alpha_{95} = 31$) and a positive baked contact test. McElhinny and Evans (1976) viewed the remanence as primary, implying a palaeolatitude of $1 \pm 17°$ for intrusion. The abnormally scattered directions were ascribed to a weak geomagnetic field, implied by a low ratio of natural remanent magnetisation to laboratory thermoremanent magnetisation.

Li (2000) collected 55 samples of red siltstone and mudstone from seven sites in the low-dipping Elgee Siltstone of the upper Kimberley Group (Table 1) in the southeastern Kimberley Basin (latitude 18.4°S, longitude 126.6°E; Fig. 1). The rocks contained an extremely stable remanence carried by hematite (unblocking temperature >600 °C), with a direction of declination $D = 92.2°$, inclination $I = 14.9°$ ($\alpha_{95} = 6.4°$). Although lack of suitable structure did not allow a fold test to be executed, Li (2000) interpreted the remanence as primary because of its extreme stability, the dissimilarity of the determined direction from expected younger remanence directions, and the absence of regional overprint in the nearby Hart Dolerite. The study of Li (2000) suggested that the Elgee Siltstone was deposited in low palaeolatitudes (7.6 +3.4/−3.3°).

The apparent polar wander path (APWP) for the Australian Precambrian (Schmidt and Clark, 1994; Idnurm et al., 1995; Li, 2000; Williams et al., 2004) is consistent with northwestern Australia occupying low palaeolatitudes at 1.8 Ga. However, the absence of a positive palaeomagnetic field test for the Kimberley Group and the widely scattered mean directions for the Hart Dolerite together indicated the need for more and better palaeomagnetic data from the Kimberley Group.

5. New palaeomagnetic data

5.1. Sampling sites

Red beds from the Kimberley Group were sampled by us in the northeastern Kimberley Basin (Figs. 1 and 4) 350 km northeast of

Table 2
Palaeomagnetic summary for the Elgee Siltstone (mean site λ_s = 15.7°S, φ_s = 128.3°E).

Site	*n*/no	D_h (°)	I_h (°)	DDA/dip (°)	D_b (°)	I_b (°)	α_{95} (°)	*k*
This study								
KE01	6/6	101.0	0.6	268/15	101.5	15.2	4.6	215
KE02	6/6	92.2	13.6	268/15	92.6	28.6	7.2	88
KE03	5/6	90.5	−5.8	273/11	90.5	5.2	1.8	1826
KE04	6/6	96.5	−4.7	273/11	96.5	6.3	6.4	110
KE05	6/6	95.9	0.9	281/13	95.7	13.8	6.2	119
Mean	*N* = 5	95.2	0.9		95.4	13.8		
		k = 87	α_{95} = 8.3°		*k* = 63	α_{95} = 9.7°		
Li (2000)†								
KE01	8/10	94.7	12.7	009/19	90.8	10.6	10.4	29
KE02	13/14	91.4	11.8	009/19	88.0	8.7	8.1	27
KE03	8/8	99.7	16.0	322/13	96.3	25.4	7.4	57
KE04	9/10	92.3	2.5	338/19	90.4	10.1	8.3	39
KE05	5/5	95.8	8.9	261/15	97.0	23.4	3.6	457
KE06	4/4	89.5	7.3	243/11	90.6	17.1	7.7	143
KE07	4/4	92.3	24.8	340/8	88.6	27.6	5.4	288
Mean	*N* = 7	93.7	12.0		91.6	17.6		
		k = 108	α_{95} = 5.8°		*k* = 89	α_{95} = 6.4°		
Overall	*N* = 12	94.3	7.4		93.2	16.0		
		k = 70	α_{95} = 5.2°		*k* = 77	α_{95} = 5.0°		

DDA, down-dip azimuth of bedding; *n*/no, number of specimens showing the characteristic remanence/total number of specimens; *N*, number of sites; α_{95}, half-angle of the 95% confidence cone for the mean direction; D_h and I_h, *in situ* declination and inclination; D_b and I_b, declination and inclination with respect to bedding; *k*, precision parameter of Fisher (1953) distribution for mean directions; d_p, d_m, semi-axes of error ellipse around the pole of probability of 95%.

† Directions from Li (2000) have been recalculated for the mean site here, λ_s = 15.7°S, φ_s = 128.3°E. Dip-corrected pole position: λ_p = 5.2°S, φ_p = 211.2°E, d_p = 2.6°, d_m = 5.1°.

the sampling area of Li (2000). Three block samples were collected at each of five sites in the low-dipping Elgee Siltstone, and three block samples at each of eight sites in the low- to moderate-dipping, lower and middle members of the Pentecost Sandstone. The site localities are shown in Fig. 4 and details given in Appendix A. The Hart Dolerite does not crop out in the sampling areas.

We also took 51 block and core samples of tholeiitic basalt from the Carson Volcanics at 13 sites in the central Kimberley region near the Gibb River Road between 16°37′S, 126°00′E and 16°19′S, 126°30′E (Mount Elizabeth 1:250,000 Geological Sheet; Roberts et al., 1966). Twenty-four block samples of red brown, locally micaceous sandstone from the Lansdowne Arkose were collected at eight sites in a road cut on the Great Northern Highway at 15°57.9′S, 128°25.3′E (Cambridge Gulf 1:250,000 Geological Sheet; Plumb and McGovern, 1968). In addition, 114 block and core samples of the Hart Dolerite were collected at 20 sites in the southwestern Kimberley region between 16°47′S, 124°55′E and 17°11′S, 125°15′E (Lennard River and Charnley 1:250,000 geological sheets; Gellatly and Halligan, 1971; Griffin et al., 1993). Details of all these sites are given in Appendix A.

The samples were oriented with both sun and magnetic compasses. The mean of the local declination agreed within error with the published value of 3° except near some sites in the Carson Volcanics and Hart Dolerite where extremely strong remanent magnetisation, presumably caused by lightning, deflected the magnetic compass by >10°.

5.2. Laboratory techniques

Between three and eight specimens 2.2 cm high × 2.5 cm in diameter were machined from the block samples and at least two specimens per sample, six per site, were processed. Routine palaeomagnetic laboratory methods (Collinson, 1983; Butler, 1992) were employed. Remanent magnetisation was measured using a 2G 755R three-axis cryogenic magnetometer. The demagnetisers used were an in-line 2G 600 series AF demagnetiser and a Magnetic Measurements MMTD80 shielded furnace. All specimens were subjected to stepwise thermal demagnetisation. Prior to thermal demagnetisation, specimens of igneous rocks were subjected to low-temperature pretreatment (Schmidt, 1993).

Table 3
Palaeomagnetic summary for the Pentecost Sandstone characteristic remanent magnetisation (ChRM) (mean site λ_s = 15.7°S, φ_s = 128.3°E) plus the combined result for all red beds.

Site	*n*/no	D_h (°)	I_h (°)	DDA/dip (°)	D_b (°)	I_b (°)	α_{95} (°)	*k*
KP01	4/6	104.0	42.7	138/27	112.2	19.1	9.5	95
KP02†	*2/6*	*81.6*	*15.1*	*126/26*	*83.4*	*−3.2*	–	–
KP05	6/6	89.7	18.4	63/8	88.8	11.2	5.7	139
KP06	7/7	88.9	23.6	83/6	88.7	17.6	9.7	40
KP07	5/6	86.3	31.1	68/20	84.0	12.0	13.9	31
KP08	6/6	96.9	15.5	117/12	97.6	4.2	5.4	155
Mean	*N* = 5	92.8	26.4		94.1	13.0		
		k = 42	α_{95} = 11.9°		*k* = 43	α_{95} = 11.7°		
Overall	*N* = 17	93.9	12.9		93.5	15.1		
Elgee and Pentecost		*k* = 36	α_{95} = 6.0°		*k* = 67	α_{95} = 4.4°		

Dip-corrected pole position: λ_p = 5.4°S, φ_p = 211.8°E, d_p = 2.3°, d_m = 4.5°. See Table 2 for explanation of abbreviations.

† Site KP02 omitted from mean because only two specimens yielded ChRM directions.

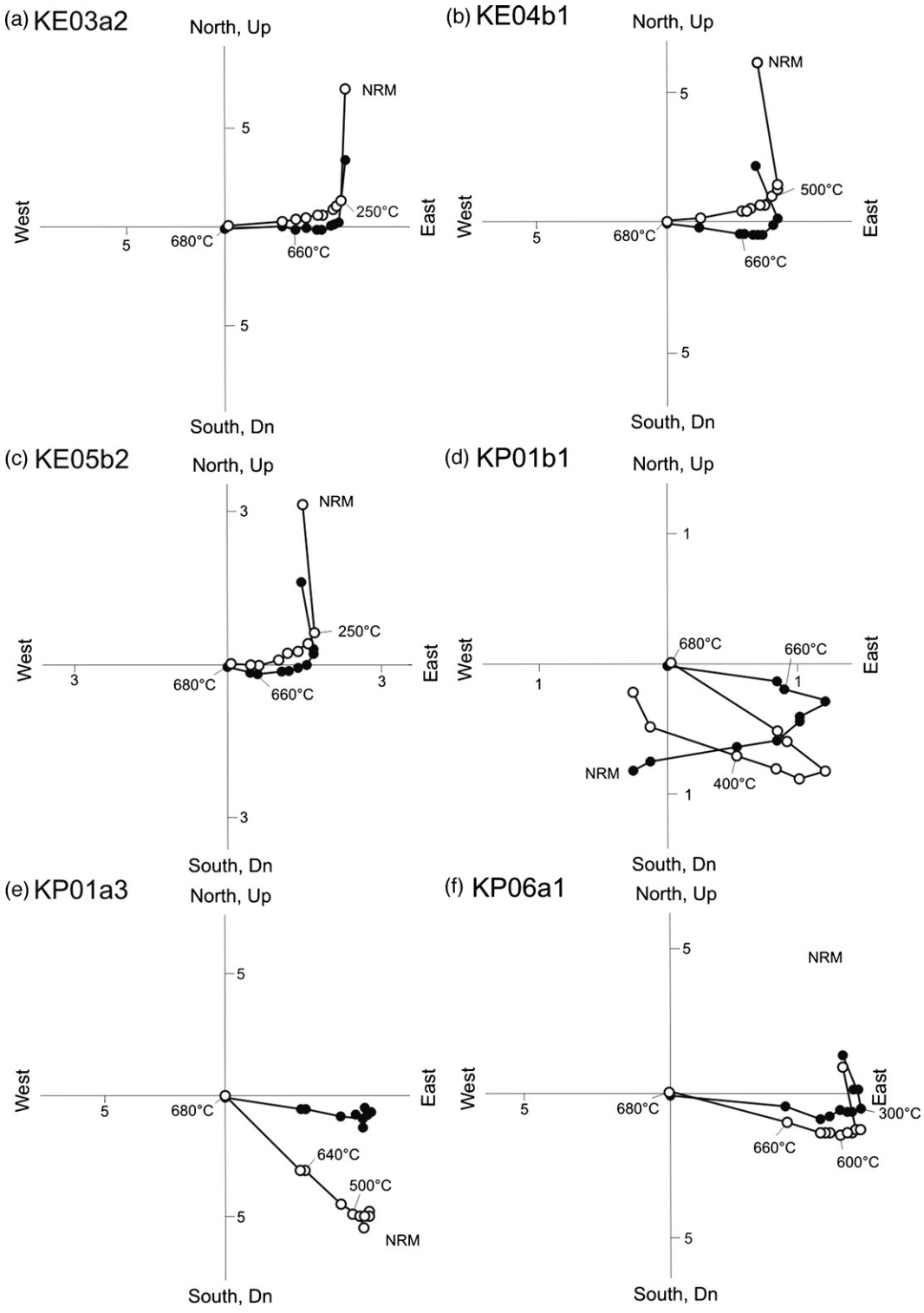

Fig. 5. Orthogonal projections of remanence vectors after stepwise thermal demagnetisation (°C). Solid circles plot on the horizontal plane and open circles on the vertical plane. Axes are mA m^{-1} (10^{-6} emu/cc). KE, specimens from the Elgee Siltstone; KP, specimens from the Pentecost Sandstone. See text for details.

Stepwise AF demagnetisation was also applied to the igneous specimens.

Magnetisation components were isolated using an interactive version of Linefind (Kent et al., 1983), in which linear segments are fitted to data points weighted according to the inverse of their measured variances. The highest temperature to which any particular component remains stable, i.e. the highest unblocking temperature observed, was generally taken as an indication of the Curie temperature of the mineral carrying that component.

5.3. Results

Our results are summarised in Tables 2 and 3. Orthogonal projections of the demagnetisation vectors for both the Elgee Siltstone

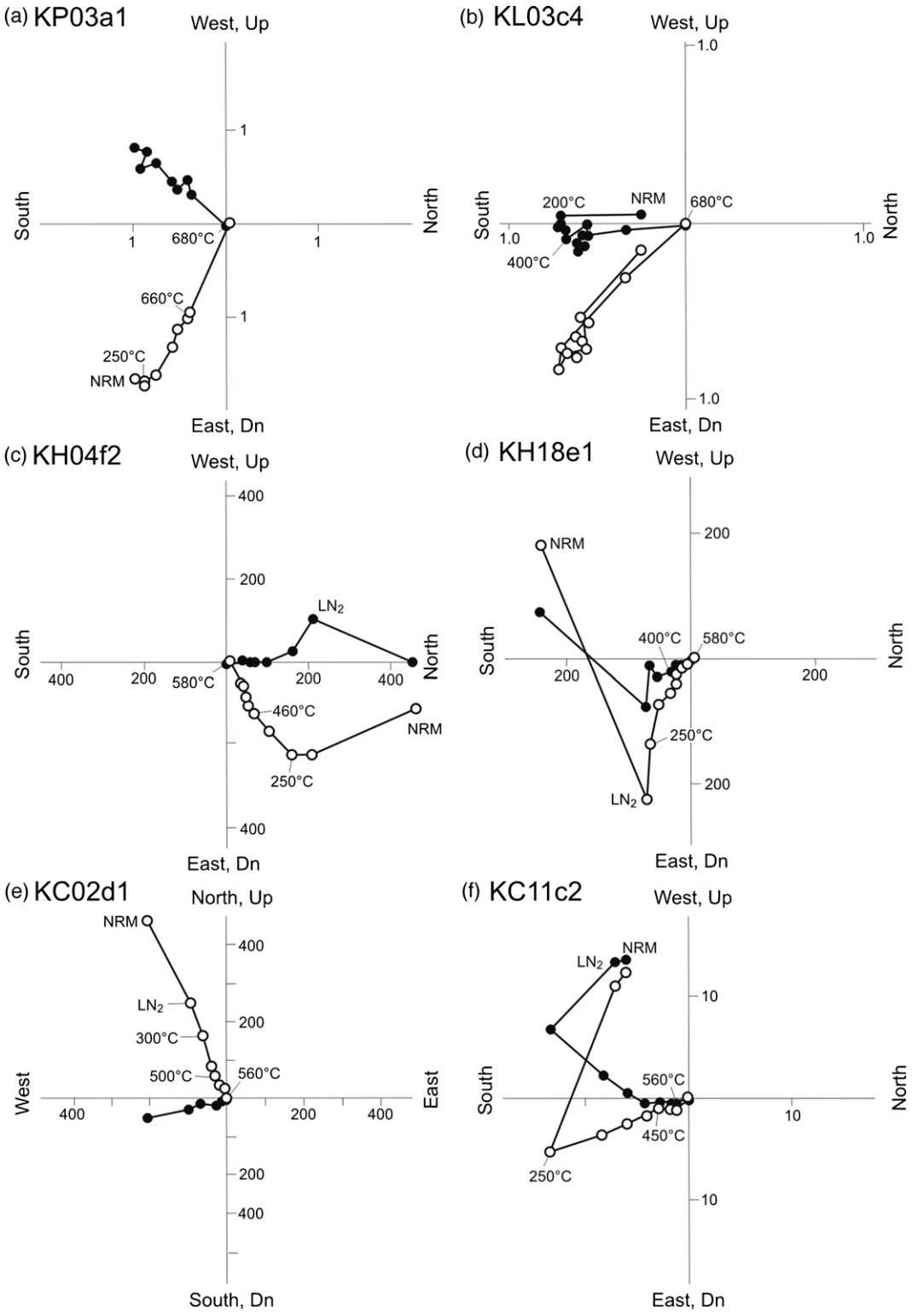

Fig. 6. Orthogonal projections of remanence vectors after stepwise thermal demagnetisation (°C). Solid circles plot on the horizontal plane and open circles on the vertical plane. Axes are mA m^{-1} (10^{-6} emu/cc). KP, Pentecost Sandstone; KL, Lansdowne Arkose; KH, Hart Dolerite; KC, Carson Volcanics. See text for details.

and Pentecost Sandstone generally show two components (Fig. 5). A viscous component closely aligned with the local geomagnetic field was removed below 300 °C, leaving a component with a higher unblocking temperature that is shallowly inclined to the east and that is not completely erased until 690 °C. The high unblocking temperature indicates that the stable component is carried by hematite.

Specimens such as KP01b1 (Fig. 5d) from the Pentecost Sandstone display two almost antiparallel components, of which the more stable conforms to that of other specimens. The less

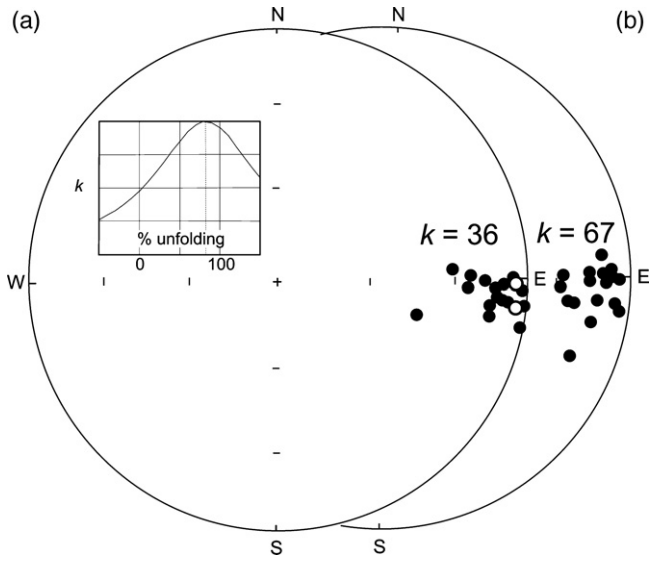

Fig. 7. Stereographic projections of site mean ChRM directions for the Elgee Siltstone and Pentecost Sandstone, including those of Li (2000) for the Elgee Siltstone (after conversion to the mean site locality of the present study; see Table 2), isolated by stepwise thermal demagnetisation. Solid circles plot on the lower hemisphere and open circles on the upper hemisphere: (a) present-day coordinates, and (b) after unfolding. The tighter cluster of the latter reflects a fold test at 99% confidence.

stable component is inclined shallowly to the west, suggesting that the magnetisation is a chemical remanent magnetisation (CRM) acquired over a time comparable to the ancient geomagnetic reversal rate.

Orthogonal projections of the demagnetisation vectors for weathered Pentecost Sandstone and Lansdowne Arkose are shown in Fig. 6a and b, respectively. These components are close to the reverse polarity late Tertiary geomagnetic field direction for the region, in sharp contrast to the easterly directions clearly seen for unweathered samples. The alteration is not easily detected by visual inspection in the field. Orthogonal projections also are shown for the Hart Dolerite and Carson Volcanics (Fig. 6c–f), for which no characteristic remanent magnetisation (ChRM) could be identified.

Results for five sites (29 specimens) in the Elgee Siltstone southeast of Wyndham (Fig. 4) gave a dip-corrected mean direction of $D = 95.4^\circ$, $I = 13.8^\circ$ ($\alpha_{95} = 9.7^\circ$), implying a palaeolatitude $\lambda = 7.0$ +5.3/−5.0°. Results for five sites (28 specimens) from the Pentecost Sandstone gave a dip-corrected mean direction of $D = 94.1^\circ$, $I = 13.0^\circ$ ($\alpha_{95} = 11.7^\circ$), $\lambda = 6.6$ +6.4/−5.9°. One site (KP02) for which only two specimens possessed the easterly component has been neglected. Combining our data for the Elgee Siltstone and Pentecost Sandstone with the results for the seven sites in the Elgee Siltstone determined by Li (2000) yields a dip-corrected mean direction of $D = 93.5^\circ$, $I = 15.1^\circ$ ($\alpha_{95} = 4.4^\circ$), $\lambda = 7.7 \pm 2.3^\circ$, and a pole position at latitude $\lambda_p = 5.4^\circ$S, longitude $\varphi_p = 211.8^\circ$E, with confidence semi-axes $d_p = 2.3^\circ$ and $d_m = 4.5^\circ$.

Site mean ChRM directions for the Elgee Siltstone and Pentecost Sandstone, including those of Li (2000) for the Elgee Siltstone (after conversion to the mean site locality of the present study to allow them to be included in a fold test; see Table 2), are shown before and after correction for bedding dip (Fig. 7a and b, respectively). The distribution of directions before correction is distinctly elongated in the plane containing the bedding pole and the dip azimuth, whereas the distribution after correction appears to be more Fisherian. To test the magnetic age with respect to folding, the directions were analysed using the fold test of McFadden (1990). Employing the first convention of McFadden (1990), designed for comparable situations where the mean directions before and after unfolding are similar, the 95 and 99% confidence correlation values for 17 sites are 4.801 and 6.721, respectively. The correlation values before and after correction for the 17 site mean directions analysed here are 8.575 and 4.721, respectively, indicating that the bedding structure is correlated with the directional distribution before correction but has no apparent correlation after correction. The correlation is sufficiently significant before correction as to indicate a positive fold test at 99% confidence.

It is noteworthy that a positive fold test also is achieved without including the directions of Li (2000). For the five Elgee Siltstone sites and five Pentecost Sandstone sites we report here, the 95 and 99% confidence correlation values (for 10 sites) are 3.685 and 5.120, respectively, while the observed correlation values before and after correction for the 10 site mean directions are 7.602 and 0.865, respectively, indicating high correlation before unfolding and negligible correlation after unfolding. This is again positive with 99% confidence, but for completeness we choose to include the directions of Li (2000) in our analysis.

Components of magnetisation found in two sites out of eight (KP03 and KP04) for the Pentecost Sandstone yielded *in situ* directions of $D = 204.0^\circ$, $I = 58.4^\circ$ ($\alpha_{95} = 6.0^\circ$), and a pole position at latitude $\lambda_p = 58.5^\circ$S, longitude $\varphi_p = 91.0^\circ$E ($d_p = 6.5^\circ$ and $d_m = 8.8^\circ$). Similarly, analysis of components found in the Lansdowne Arkose yielded directions from 17 specimens of $D = 186.0^\circ$, $I = 53.4^\circ$ ($\alpha_{95} = 8.4^\circ$), and a pole position at latitude $\lambda_p = 70.9^\circ$S, longitude $\varphi_p = 112.8^\circ$E ($d_p = 8.1^\circ$ and $d_m = 11.6^\circ$). The unblocking temperatures of these components were distributed from low temperatures up to the Curie temperature for hematite (685 °C), and completely masked the easterly directed component. The masking of earlier components is typical of rocks that have been exposed to deep tropical weathering (Schmidt and Embleton, 1976; Idnurm and Senior, 1978).

ChRM directions for the Carson Volcanics and Hart Dolerite were scattered. Some of the Carson Volcanics and Hart Dolerite sites have been affected by lightning strikes, as inferred from magnetic compass needle deflections at the sites, but not all the scatter can be ascribed to this source. The tholeiitic basalts of the Carson Volcanics are mostly altered to spilite (Plumb and Gemuts, 1976; Griffin and Grey, 1990) and hence the magnetite would not be magmatic and therefore would not retain a thermoremanent magnetisation. The very weak magnetisation displayed by the Hart Dolerite also may result from spilitisation. Directions after demagnetisation and principal component analysis are plotted for specimens of both the Hart Dolerite and the Carson Volcanics that possessed Königsberger (Q) ratios <10 to minimise the effects of lightning (Fig. 8). Some specimens from both units possessed $Q > 100$. For the Hart Dolerite just 77 out of a total of 123 treated specimens, and for the

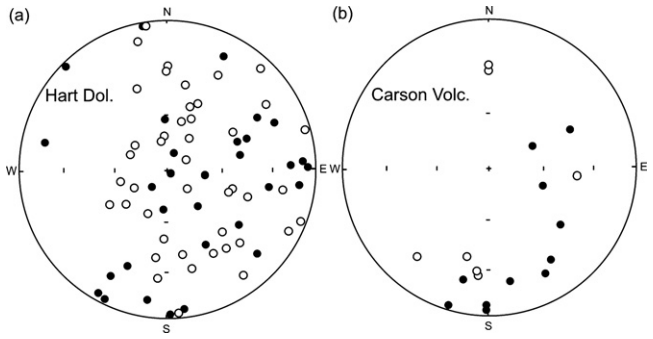

Fig. 8. Stereographic projections of directions after demagnetisation and principal component analysis for specimens from (a) the Hart Dolerite and (b) the Carson Volcanics which possessed Königsberger (Q) ratios <10 and are thought to be least affected by lightning. See text for details.

Carson Volcanics only 18 out of a total of 95 treated specimens, survived this low pass Q-filter. Both units yielded highly scattered directions that defy further analysis. McElhinny and Evans (1976) studied the Hart Dolerite and Carson Volcanics in the southeastern Kimberley region so our results for the southwestern and central Kimberley region may not bear on their findings, although we note that they found Hart Dolerite directions were rather scattered with $\alpha_{95} = 31^\circ$ for 12 sites, and Carson Volcanics directions, as herein, were uninterpretable.

5.4. Interpretation of results

The basinwide agreement of results for the Elgee Siltstone and the positive fold tests for the combined data for the Elgee Siltstone and Pentecost Sandstone argue strongly for early acquisition of the stable magnetisation. The evidence for reversals in some specimens is consistent with the magnetisation being a CRM acquired close to the time of deposition.

Tectonic events that have affected Proterozoic strata in the Kimberley region, including different parts of the Kimberley Group at different times, are:

(1) Folding, uplift and erosion of the Kimberley Group in the northeastern Kimberley Basin estimated at ~1790–1750 Ma, prior to deposition of the unconformably overlying Bastion Group (Thorne et al., 1999). The age of initial deformation of the Kimberley Group was based on a whole-rock Rb–Sr isochron indicating an apparent age of 1789 ± 58 Ma for the Wyndham Shale of the Bastion Group (Bofinger, 1967). A late Palaeoproterozoic age for this deformation is supported by the correlation of the Bastion Group with the Birrindudu Group in the Birrindudu Basin (Fig. 1; Hendrickx et al., 2000), whose age is given as between 1790 and 1700 Ma (Hendrickx et al., 2000) and between 1735 and 1640 Ma (Crispe et al., 2007). This deformation may be coeval with the Yapungku Orogeny (1.79–1.76 Ga) in north-central Western Australia (Bagas, 2004; Pirajno et al., 2004).
(2) Folding, uplift and erosion of the Bastion Group at 1550–1250 Ma, prior to deposition of the Mesoproterozoic Carr Boyd Group (Thorne et al., 1999).
(3) Yampi Orogeny at ~1000 Ma in the west Kimberley region (Thorne et al., 1999). Biotite K–Ar ages for sheared granitoid rocks from the Hooper Complex place age limits of 1475 ± 12 and 999 ± 9 Ma on this orogeny (Shaw et al., 1992).
(4) Neoproterozoic King Leopold Orogeny (Griffin et al., 1993; Thorne et al., 1999). This produced extensive west-northwesterly trending folds and thrusts in the King Leopold Ranges along the southwestern margin of the Kimberley Basin, reactivated shear zones in the Hooper Complex, and caused sinistral strike-slip faulting in the Halls Creek Orogen (Tyler et al., 1991; Shaw et al., 1992).

Li (2000) equated the age of remanence acquisition of the Elgee Siltstone with the diagenetic xenotime ages of 1704 ± 7 and 1704 ± 14 Ma for the bounding Warton Sandstone and Pentecost Sandstone, respectively (Fig. 2). However, the xenotime ages are ~100 million years younger than the age of deposition. This and the agreement of the Warton and Pentecost xenotime results suggest that the ages do not record early diagenesis, when red beds like the Elgee Siltstone and Pentecost Sandstone usually acquire an early CRM (Turner, 1980). A late Palaeoproterozoic (~1.79–1.75 Ga) age for initial uplift and folding of the Kimberley Group in the northeastern Kimberley Basin, if confirmed, would suggest that the xenotime ages of 1704 Ma for the Warton Sandstone and Pentecost Sandstone were set after the Kimberley Group was moderately folded and uplifted, eroded and then buried by the Bastion Group.

Thin sills of Hart Dolerite intrude the formations up to the top of the Kimberley Group, including the Elgee Siltstone and Pentecost Sandstone (Gellatly et al., 1975; Griffin et al., 1993). Hence the Elgee Siltstone and Pentecost Sandstone are older than 1790 ± 4 Ma, which does not conflict with the detrital zircon ages (Fig. 2). As noted above, a positive fold test is achieved using only our 10 sites in the Elgee Siltstone and Pentecost Sandstone in the northeastern Kimberley Basin. This region in particular was affected by the ~1.79–1.75 Ga folding, so the positive fold test probably relates in large part to that deformation. However, we cannot exclude the possibility that the fold test relates in part to Mesoproterozoic deformation. Nonetheless, the basinwide concordance of palaeomagnetic results for the Elgee Siltstone, and the positive fold test coupled with the evidence for deformation at ~1.79–1.75 Ga in our sampling area, argue for an early magnetisation.

Taking the age of the Elgee magnetisation as close to the time of deposition and possibly older than 1790 Ma implies a short time interval between the King Leopold glaciation at ~1800 Ma and Elgee–Pentecost remanence acquisition. This further implies that the King Leopold glaciation occurred at a low palaeolatitude ($\lambda = 8 \pm 2^\circ$). In addition, the pole position for the 1822 Ma Plum Tree Creek Volcanics in the Pine Creek Orogen (Idnurm and Giddings, 1988; Kruse et al., 1994; Idnurm, 2004) falls at 29°S, 195°E (Fig. 9), yielding a palaeolatitude of 28° at 1822 Ma for the mean site locality studied here and confirming the presence of northwestern Australia in low palaeolatitudes during the late Palaeoproterozoic.

As noted above, the Lansdowne Arkose and some samples from the Pentecost Sandstone yielded directions that are close to the late Tertiary geomagnetic field direction for the region. These directions comprise both normal and reverse polarities, reminiscent of those found in many regolith profiles across Australia (Schmidt and Embleton, 1976; Schmidt et al., 1976; Idnurm and Senior, 1978), and are interpreted to reflect weathering and lateritisation related to regolith formation. Schmidt and Williams (2002) and Williams et al. (2004) found similar directions in weathered material below the Older Plateau surface in Western Australia, where $D = 183.5^\circ$, $I = 55.3^\circ$ ($\alpha_{95} = 5.3^\circ$). In that instance the number of normal directions and reverse directions was almost equal and the pole position is located at latitude $\lambda_p = 80.0^\circ$S, longitude $\varphi_p = 105.3^\circ$E ($d_p = 5.3^\circ$, $d_m = 7.5^\circ$), not significantly different from the pole calculated here for the Lansdowne Arkose (latitude $\lambda_p = 70.9^\circ$S, longitude $\varphi_p = 112.8^\circ$E, $d_p = 8.1^\circ$ and $d_m = 11.6^\circ$). Our study adds to the palaeomagnetic database for Australia's regolith and a more complete analysis will be reported elsewhere.

6. Discussion

6.1. Continental assembly

The King Leopold glaciation was initiated on the Halls Creek Orogen to the east of the Kimberley Basin (Fig. 1) following collision of the Kimberley Craton and the North Australian Craton at ~1820 Ma (Page et al., 2001; Tyler et al., 2005). This collision was part of the worldwide assembly of a pre-Rodinia supercontinent at ~1.8 Ga – "Columbia" of Zhao et al. (2002, 2004) and "Hudsonland" of Pesonen et al. (2003) – and Tyler et al. (2005) suggested that the Halls Creek Orogen may represent part of a larger collisional orogen comparable in scale to the Alpine–Himalayan Orogen. Deformation and metamorphism in the Halls Creek Orogen ended by ~1815 Ma, and post-collisional granite intrusion occurred widely from ~1820 to1805 Ma (Page et al., 2001; Sheppard et al., 2001). Net vertical displacement of 2–6 km of metamorphic rocks in the central

part of the orogen took place across the post-1820 Ma Highway Shear Zone (Bodorkos and Reddy, 2005). The occurrence of the King Leopold glaciation suggests that major uplift of the Halls Creek Orogen accompanied this post-collisional diastrophism, with maximum uplift recorded by glaciation in the adjacent Kimberley Basin at ~1800 Ma.

An updated APWP for late Palaeoproterozoic rocks of the West Australian Craton, including the Earaheedy Group in the Earaheedy Basin, and the North Australian Craton is shown in Fig. 9. Pirajno et al. (2004) concluded that the Earaheedy Group is younger than 1.84 Ga and probably older than the Yapungku Orogeny at 1.79–1.76 Ga. They further concluded that the Stanley folding of the Earaheedy Group was coeval with the D_2 phase of the Yapungku Orogeny, thought to record the collision of the West Australian and North Australian cratons. Halilovic et al. (2004) discussed age constraints on the Earaheedy Group and reached a similar conclusion. It follows that the Kimberley and Earaheedy groups are broadly coeval and that deformation of the Earaheedy Group occurred at about the same time as the initial uplift and folding of the Kimberley Group, during cratonic collision. Whereas palaeomagnetic inclinations for the Frere Formation of the Earaheedy Group (Williams et al., 2004) and the Elgee–Pentecost of the Kimberley Group are similar, their declinations are different. The 45° separation between the Frere and Elgee–Pentecost poles (FFA, FFB and EP, EG, respectively; Fig. 9) reflects this difference in declination and represents relative rotation about a vertical axis during or after the Yapungku Orogeny. Schmidt et al. (2006) noted discrepancies among the poles for the 1.07 Ga Warakurna Igneous Province (Wingate et al., 2004), namely those for the Bangemall Supergroup sills from the West Australian Craton and the Stuart Dykes and Alcurra Dyke Swarm from the North Australian Craton, suggesting that a merger of the cratons at 1.79–1.76 Ga was temporary and followed by separation before final assembly after 1.07 Ga.

6.2. Palaeolatitude and palaeogeography of Palaeoproterozoic glaciations

Our palaeomagnetic data imply that the Kimberley Group was deposited near the palaeoequator ($8 \pm 2°$ palaeolatitude) and that the late Palaeoproterozoic King Leopold glaciation occurred in low palaeolatitudes. The presence of sandstone-filled frost fissures in the Bedford surface indicates a frigid, periglacial climate, with temperatures possibly as low as −20 °C near sea level (Williams, 2005). Hence the enigma of glaciation and cold climate near sea

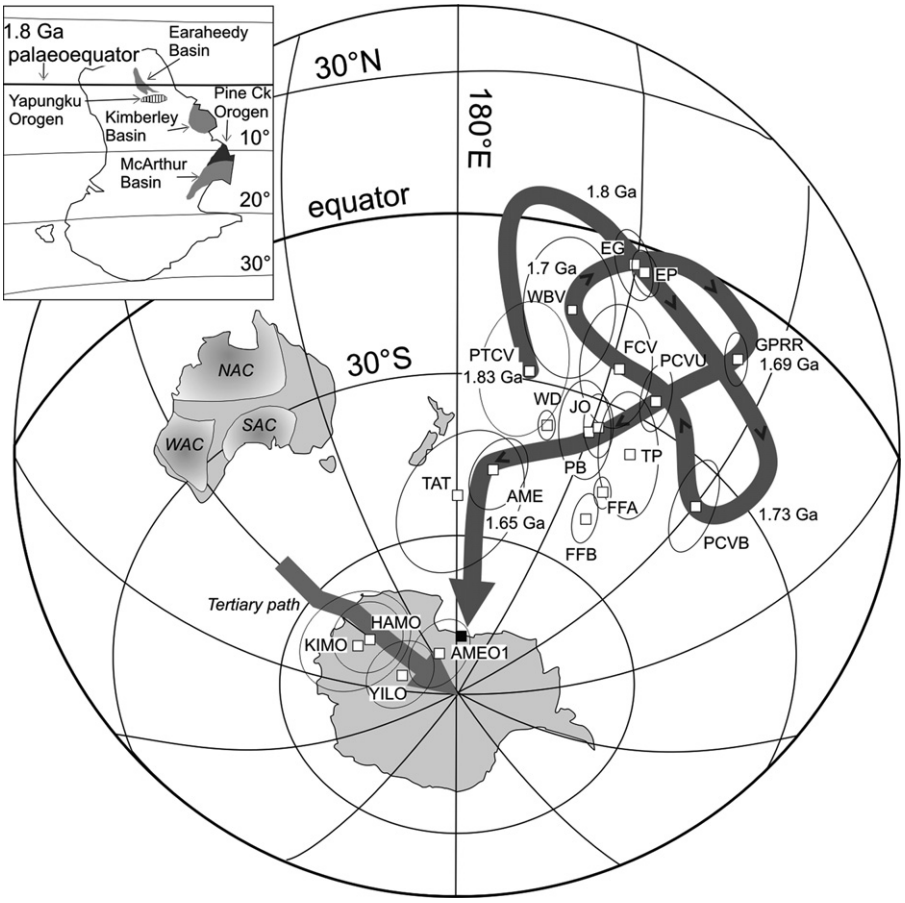

Fig. 9. Updated APWP for the late Palaeoproterozoic of western and northern Australia. EP, palaeomagnetic poles for combined Elgee Siltstone–Pentecost Sandstone (herein); WD, Wittenoom Dolomite (Li et al., 1993); FFA and FFB, Frere Formation components A and B, respectively (Williams et al., 2004); JO, late to post-Capricorn overprint poles for Mount Jope Volcanics, southern Pilbara Craton (Schmidt and Embleton, 1985); PB, Paraburdoo hematitic ore-body (Schmidt and Clark, 1994); TP, Tom Price hematitic ore-body (Schmidt and Clark, 1994). Other late Palaeoproterozoic poles for northern Australia: EG, Elgee Siltstone (Li, 2000); PCVB and PCVU, basalt near base and top of Peters Creek Volcanics, respectively; GPRR, Gunpowder Creek Formation; FCV, Fiery Creek Volcanics; WBV, West Branch Volcanics; AME, Amelia Dolomite; TAT, Tatoola Sandstone (all from Idnurm, 2000); PTCV, Plum Tree Creek Volcanics (Idnurm and Giddings, 1988; Idnurm, 2004). Polarities are not implied. NAC, North Australian Craton; SAC, South Australian Craton; WAC, West Australian Craton. The Tertiary APWP for Australia is shown as a light-toned track along with regolith poles from highly weathered material beneath the Hamersley Surface, HAMO (Schmidt and Williams, 2002), below the Older Plateau surface on the edge of the Yilgarn Craton, YILO (Williams et al., 2004), and weathered Lansdowne Arkose, KIMO (herein). The remaining poles represent an overprint pole for the Amelia Dolomite, AMEO1 (Idnurm, 2000) that we suggest is of Tertiary age; the pole using *in situ* directions (white square) falls closer to the Tertiary APWP.

level in low palaeolatitudes, which marks the Neoproterozoic (e.g. Schmidt and Williams, 1995; Park, 1997; Evans, 2000; Williams and Schmidt, 2004) and early Palaeoproterozoic (e.g. Evans et al., 1997; Williams and Schmidt, 1997; Schmidt and Williams, 1999), evidently applies also to the late Palaeoproterozoic.

The King Leopold glaciation appears to have been a brief event, albeit deep within the tropics. The wide extent of the Emu Point Member implies the presence of an ice cap on the elevated Halls Creek Orogen rather than restricted mountain glaciation. Indeed, the Halls Creek Orogen may have undergone major glaciation around 1.8 Ga, but the record of glaciation near Lansdowne in the southeastern Kimberley Basin implies a short-lived advance of grounded ice, with glacial erosion and glaciofluvial deposition near its distal margin. The presence of ventifacts in the Emu Point Member points to a windy and probably an arid periglacial climate in northwestern Australia at 1.8 Ga (Williams, 2005). Eriksson and Simpson (1998) identified a temporal concentration of Precambrian aeolianites at 1.8 Ga, suggesting that the newly assembled and locally glaciated late Palaeoproterozoic supercontinent experienced widespread aridity.

The relative fall of sea level that accompanied the King Leopold glaciation and the immediately following marine transgression across northern Australia (Williams, 2005) may have been partly glacio-eustatic, suggesting that glaciation at 1.8 Ga may have occurred elsewhere. As one example, the ~1800 Ma Reynolds Range Group in central Australia commences with a 1–15 m thick, matrix-supported polymict conglomerate (Dirks, 1990; Dirks and Norman, 1992) that may prove to be of glacial origin, followed by marine transgression. However, no possible glaciogenic deposit that is correlative with the Emu Point Member has been identified elsewhere (Eriksson et al., 2005). The final stages of global continental assembly near 1.8 Ga, with shrinking seaways and widespread aridity, may have been unfavourable for the accumulation and preservation of thick glaciogenic successions. By contrast, the early Palaeoproterozoic (2.4–2.3 Ga) Huronian glaciations in Canada occurred during breakup of the end-Archaean supercontinent "Kenorland", involving rifting and ocean opening with development of a passive margin marked by deposition of the Huronian Supergroup (Young et al., 2001; Young, 2004).

The apparent brevity of the King Leopold glaciation and its associated periglacial climate near sea level, the absence of "cap carbonate" rocks, and the lack of proven coeval glaciogenic deposits elsewhere in Australia and on other continents, conflict with a postulated frozen-over Earth and other aspects of the "snowball Earth" hypothesis for low-palaeolatitude glaciation (e.g. Hoffman and Schrag, 2002). Hence it cannot be argued that the occurrence of low-palaeolatitude glaciation near sea level in the Kimberley Basin implies the late Palaeoproterozoic was a time of global freeze-over. Other explanations of Proterozoic glaciation and cold climate near sea level in low palaeolatitudes should be considered (e.g. Williams and Schmidt, 2004; Williams, 2008).

In a study similar to the present investigation, red beds from the upper Huronian Lorrain Formation, which conformably overlies the ~2.3 Ga glaciogenic Gowganda Formation in Canada, yielded a stable CRM with shallow inclinations consistent with a low palaeolatitude for the Lorrain Formation and the Gowganda glaciation (Williams and Schmidt, 1997; Schmidt and Williams, 1999). Although a fold test for the Lorrain Formation was inconclusive because of the lack of sufficient structural variation among our 17 sites, the Lorrain pole plots on an uncomplicated APWP in sequence with poles for Palaeoproterozoic (2.45–2.22 Ga) dyke swarms of the Superior Craton, which were intruded at low palaeolatitudes (Buchan et al., 1996, 1998, 2000; Williams and Schmidt, 1997; Schmidt and Williams, 1999). Hilburn et al. (2005), however, claimed a negative fold test for a small fold at one site in the Lorrain Formation. They conceded (p. 320) that the origin of the fold is "uncertain", although their observation that the fold formed "before significant vertical compaction" suggests it developed prior to significant burial and early diagenesis. Hilburn et al. (2005) further conceded that they were unable to completely resolve the stable, shallow component of Williams and Schmidt (1997), which was not expressed at all 17 sites, so the directions for the single site of Hilburn et al. (2005) are likely to be contaminated with one or more of the many overprints carried by the Lorrain Formation. The fold test of Hilburn et al. (2005) therefore is inconclusive and does not negate the conclusion of Williams and Schmidt (1997) that the Lorrain Formation carries a stable, shallow CRM acquired during early diagenesis and that the Gowganda glaciation likely occurred in low palaeolatitudes. It is noteworthy that the Gowganda Formation, like the Emu Point Member of the King Leopold Sandstone, lacks a cap carbonate (Young et al., 2001; Young, 2004).

6.3. Comparison with palaeomagnetic results for the McArthur Basin

Palaeomagnetic data for red beds from the late Palaeoproterozoic McArthur Basin in northern Australia are employed in the Australian Palaeoproterozoic–Mesoproterozoic APWP (Idnurm et al., 1995; Idnurm, 2000), which shows two excursions into present-day high latitudes. On the basis of our results for the Kimberley region, we query the antiquity of those high-latitude poles, principally because the Pentecost Sandstone yielded two distinct groupings of magnetisation, one pre-folding and another similar to Tertiary poles for northern Australia and close to the present-day pole. As discussed in Section 5.4, Tertiary remagnetisation through deep weathering and lateritisation of older rocks is widespread across Australia (Schmidt and Embleton, 1976; Schmidt et al., 1976; Idnurm and Senior, 1978), particularly in the tropics, and sites in gullies and road cuts commonly are not far below the surface of deeply weathered and now partly dissected Mesozoic–Tertiary peneplains. Rather than the late Palaeoproterozoic–Mesoproterozoic APWP for northern Australia making excursions into present-day high latitudes, those high-latitude poles should be assigned to Australia's Tertiary APWP.

7. Conclusions

Palaeomagnetic study of red beds from the ~1800–1790 Ma Kimberley Group in the northeastern Kimberley Basin, northwestern Australia, and associated sedimentary and igneous rocks, leads to the following conclusions:

- Data for the Elgee Siltstone and Pentecost Sandstone of the upper Kimberley Group, together with those of Li (2000) for the Elgee Siltstone in the southeastern Kimberley Basin, yielded a stable, high-temperature component with a mean direction of $D = 93.5^\circ$, $I = 15.1^\circ$ ($\alpha_{95} = 4.4^\circ$), $\lambda = 7.7 \pm 2.3^\circ$, and a pole position at latitude $\lambda_p = 5.4^\circ$S, longitude $\varphi_p = 211.8^\circ$E ($d_p = 2.3^\circ$ and $d_m = 4.5^\circ$).
- Our data for the Elgee Siltstone and Pentecost Sandstone satisfy a fold test at 99% confidence, as do our data combined with those of Li (2000).
- The earliest uplift and folding of the Kimberley Group in the northeastern Kimberley Basin occurred between about 1790 and 1750 Ma, prior to deposition of the unconformably overlying Bastion Group. This deformation is coeval with the Yapungku Orogeny at 1.79–1.76 Ga in north-central Western Australia, when the North Australian and West Australian cratons collided.
- The basinwide agreement of results for the Elgee Siltstone and the positive fold tests are consistent with the magnetisation of

the Elgee Siltstone and Pentecost Sandstone having been acquired soon after deposition as an early diagenetic CRM.
- Our data and those for the 1.822 Ga Plum Tree Creek Volcanics in the Pine Creek Orogen imply that northwestern Australia occupied low palaeolatitudes during the late Palaeoproterozoic.
- Equating Proterozoic palaeolatitudes with geographic latitudes (McElhinny, 2004), the 1.8 Ga King Leopold glaciation, which is recorded by a grooved pavement and glaciofluvial deposits at the base of the Kimberley Group, occurred at $8 \pm 2^\circ$ latitude.
- Results for the Carson Volcanics of the Kimberley Group and the intrusive 1.79 Ga Hart Dolerite are palaeomagnetically indecipherable and evidently reflect spilitisation after their initial cooling.
- Red beds from the Lansdowne Arkose of the underlying Speewah Group and some samples from the Pentecost Sandstone yielded directions consistent with those for late Tertiary regolith profiles elsewhere across Australia.

The King Leopold glaciation originated on the Halls Creek Orogen and extended to near sea level at the distal margin of an ice cap, where the mean annual air temperature dropped to below freezing. The enigma of glaciation and cold climate near sea level in low palaeolatitudes therefore applies not only to the Neoproterozoic and early Palaeoproterozoic but also to the late Palaeoproterozoic. However, the lack of a cap carbonate associated with deposits of the King Leopold glaciation conflicts with a pillar of the snowball Earth hypothesis for global glaciation.

The new palaeomagnetic results strongly suggest that the Palaeoproterozoic–Mesoproterozoic APWP for northern Australia (Idnurm et al., 1995; Idnurm, 2000) has no excursions into present-day high latitudes, and that the poles in present-day high latitudes are better ascribed to Tertiary regolith processes and relegated to Australia's Tertiary APWP.

Acknowledgements

We thank CSIRO Exploration and Mining, Sydney, and the Discipline of Geology and Geophysics, University of Adelaide, for providing facilities for our work. Critical comments by Keith Scott and Mike McWilliams improved the manuscript. We thank the referees, Zheng-Xiang Li and Phil McCausland, for their careful reviews.

Appendix A. Sampling sites

A.1. Elgee Siltstone

Sites KE01–KE05. Cliff on north side of Fork Creek west of the Great Northern Highway, 17 km southeast of Wyndham at 15°36.1′S, 128°13.2′E (Cambridge Gulf 1:250,000 Geological Sheet; Plumb and McGovern, 1968). Red brown siltstone, sandstone and mudstone. Down-dip azimuth (DDA) 268–281°, dip 11–15°.

A.2. Pentecost Sandstone

Site KP01. Lower/middle member (undifferentiated). Gully on west side of the Great Northern Highway 9 km north of the Dunham River, at 16°04.6′S, 128°23.8′E (Lissadell 1:250,000 Geological Sheet; Thorne et al., 1999). Rippled, red brown sandstone and red mudstone bands with desiccation cracks. DDA 138°, dip 27°.

Site KP02. Lower/middle member (undifferentiated). Trench on west side of the Great Northern Highway 11.5 km north of the Dunham River, at 16°03.4′S, 128°24.3′E (Lissadell 1:250,000 Geological Sheet; Thorne et al., 1999). Red brown and white sandstone displaying parting lineation. DDA 126°, dip 26°.

Sites KP03–KP04. Middle member. Road cut on north side of Parry Creek Road 22 km northwest of Kununurra, at 15°36.0′S, 128°38.4′E (Cambridge Gulf 1:250,000 Geological Sheet; Plumb and McGovern, 1968). Red brown sandstone. Beds near horizontal.

Sites KP05–KP06. Lower member. Road cut on west side of the Great Northern Highway 23 km southeast of Wyndham, at 15°40.1′S, 128°14.0′E (Cambridge Gulf 1:250,000 Geological Sheet; Plumb and McGovern, 1968). Red brown sandstone with local Liesegang banding. Mean attitude, DDA 73°, dip 7°.

Site KP07. Lower member. Road cut on east side of the Great Northern Highway 26 km southeast of Wyndham, at 15°41.2′S, 128°15.4′E (Cambridge Gulf 1:250,000 Geological Sheet; Plumb and McGovern, 1968). Red brown sandstone, siltstone and mudstone. DDA 68°, dip 20°.

Site KP08. Middle member. Road cut on east side of the Great Northern Highway 33 km southeast of Wyndham, at 15°44.6′S, 128°16.1′E (Cambridge Gulf 1:250,000 Geological Sheet; Plumb and McGovern, 1968). Red brown sandstone. DDA 117°, dip 12°.

A.3. Lansdowne Arkose

Sites KL01–KL08. Road cut on the Great Northern Highway 7 km south of junction with the Victoria Highway, at 15°57.9′S, 128°25.3′E (Cambridge Gulf 1:250,000 Geological Sheet; Plumb and McGovern, 1968). Red brown, locally micaceous sandstone. DDA 323°, dip 62°.

A.4. Carson Volcanics

Sites KC01–KC03. Hill on northwest side of the Gibb River Road 14 km east of Mount Barnett Roadhouse, at 16°37.5′S, 126°00.4′E (Mount Elizabeth 1:250,000 Geological Sheet; Roberts et al., 1966). Tholeiitic basalt. Regional attitude, DDA 125°, dip 10°.

Sites KC04, KC05. Hill on north side of the Gibb River Road 5.5 km west of junction with road to Mount Elizabeth, at 16°33.0′S, 126°09.4′E (Mount Elizabeth 1:250,000 Geological Sheet; Roberts et al., 1966). Tholeiitic basalt. Regional attitude, DDA 180°, dip 10°.

Sites KC06, KC07. North side of track to Gibb River Dam 2.8 km east of the Gibb River Road, at 16°25.6′S, 126°29.7′E (Mount Elizabeth 1:250,000 Geological Sheet; Roberts et al., 1966). Tholeiitic basalt. Regional attitude, DDA 135°, dip 5°.

Sites KC08, KC09. North side of track to Gibb River Dam 3.7 km east of the Gibb River Road, at 16°25.9′S, 126°30.2′E (Mount Elizabeth 1:250,000 Geological Sheet; Roberts et al., 1966). Tholeiitic basalt. Regional attitude, DDA 135°, dip 5°.

Sites KC10, KC11. East of the Gibb River Road 10.4 km north of junction with road to Gibb River (Ngallagunda), at 16°21.8′S, 126°30.5′E (Mount Elizabeth 1:250,000 Geological Sheet; Roberts et al., 1966). Tholeiitic basalt. Regional attitude, DDA 85°, dip 5°.

Sites KC12, KC13. Hill east of the Gibb River Road 16 km north of junction with road to Gibb River (Ngallagunda), at 16°18.9′S, 126°30.2′E (Mount Elizabeth 1:250,000 Geological Sheet; Roberts et al., 1966). Tholeiitic basalt. Regional attitude, DDA 85°, dip 10°.

A.5. Hart Dolerite

Sites KH1, KH2. The Barker River 1.5 km west of Mount Matthew, at 16°46.7′S, 124°54.7′E (Charnley 1:250,000 Geological Sheet; Gellatly and Halligan, 1971). Dolerite.

Sites KH3–KH5. Creek crossing with road to Mount Hart Wilderness Lodge, at 16°58.5′S, 125°02.2′E (Charnley 1:250,000 Geological Sheet; Gellatly and Halligan, 1971). Dolerite.

Sites KH6, KH7. Creek 60 and 10 m upstream from crossing with road to Mount Hart Wilderness Lodge, at 16°59.5′S, 125°05.0′E (Charnley 1:250,000 Geological Sheet; Gellatly and Halligan, 1971). Dolerite.

Site KH8. Creek 50 m downstream from crossing with road to Mount Hart Wilderness Lodge, at 16°59.5′S, 125°05.0′E (Charnley 1:250,000 Geological Sheet; Gellatly and Halligan, 1971). Dolerite.

Site KH9. Creek crossing with road to Mount Hart Wilderness Lodge, at 17°01.8′S, 125°06.8′E (Lennard River 1:250,000 Geological Sheet; Griffin et al., 1993). Dolerite.

Sites KH10–KH12. Creek crossing 20–100 m upstream from road to Mount Hart Wilderness Lodge, at 17°03.8′S, 125°10.1′E (Lennard River 1:250,000 Geological Sheet; Griffin et al., 1993). Dolerite.

Site KH13. East side of road to Mount Hart Wilderness Lodge 1.3 km by odometer north of the Gibb River Road, at 17°05.9′S, 125°11.1′E (Lennard River 1:250,000 Geological Sheet; Griffin et al., 1993). Granophyric dolerite.

Site KH14. By track to Lennard River Gorge 3.2 km by odometer south of the Gibb River Road, at 17°09.9′S, 125°13.2′E (Lennard River 1:250,000 Geological Sheet; Griffin et al., 1993). Dolerite.

Site KH15. By track to Lennard River Gorge 2.3 km by odometer south of the Gibb River Road, at 17°09.6′S, 125°13.6′E (Lennard River 1:250,000 Geological Sheet; Griffin et al., 1993). Dolerite.

Sites 16–18. North bank of the Lennard River 30–200 m southeast of track to the Gibb River Road, at 17°11.1′S, 125°15.4′E (Lennard River 1:250,000 Geological Sheet; Griffin et al., 1993). Dolerite.

Sites 19, 20. North bank of the Lennard River 100–160 m northwest of track to the Gibb River Road, at 17°11.0′S, 125°15.2′E (Lennard River 1:250,000 Geological Sheet; Griffin et al., 1993). Dolerite.

References

Bagas, L., 2004. Proterozoic evolution and tectonic setting of the northwest Paterson Orogen, Western Australia. Precambrian Research 128, 475–496.

Bodorkos, S., Reddy, S.M., 2005. $^{40}Ar/^{39}Ar$ constraints on Proterozoic cooling and exhumation of the Halls Creek Orogen, WA. Geological Society of Australia Abstracts 81, 34.

Bofinger, V.M., 1967. Geochronology of the East Kimberley area of Western Australia. PhD thesis, Australian National University, Canberra.

Buchan, K.L., Halls, H.C., Mortensen, J.K., 1996. Paleomagnetism, U–Pb geochronology, and geochemistry of Marathon dykes, Superior Province, and comparison with the Fort Frances swarm. Canadian Journal of Earth Sciences 33, 1583–1595.

Buchan, K.L., Mortensen, J.K., Card, K.D., Percival, J.A., 1998. Paleomagnetism and U–Pb geochronology of diabase dyke swarms of Minto block, Superior Province, Québec, Canada. Canadian Journal of Earth Sciences 35, 1054–1069.

Buchan, K.L., Mertanen, S., Park, R.G., Pesonen, L.J., Elming, S.-Å., Abrahamsen, N., Bylund, G., 2000. Comparing the drift of Laurentia and Baltica in the Proterozoic: the importance of key palaeomagnetic poles. Tectonophysics 319, 167–198.

Butler, R.F., 1992. Paleomagnetism: Magnetic Domains to Geologic Terranes. Blackwell, Oxford, 319 pp.

Collinson, D.W., 1983. Methods in Rock Magnetism and Palaeomagnetism. Chapman and Hall, London, 503 pp.

Crispe, A.J., Vandenberg, L.C., Scrimgeour, I.R., 2007. Geological framework of the Archean and Paleoproterozoic Tanami Region, Northern Territory. Mineralium Deposita 42, 3–26.

Crowell, J.C., 1999. Pre-Mesozoic ice ages: their bearing on understanding the climate system. Geological Society of America Memoir 192, 106.

Derrick, G.M., Gellatly, D.C., Mikolajczak, A.S., 1965. Lansdowne, W.A. Sheet SE 52-5. Bureau of Mineral Resources, Geology & Geophysics, and Geological Survey of Western Australia 1:250,000 Geological Series (http://www.ga.gov.au/map/#geology).

Dirks, P.H.G.M., 1990. Intertidal and subtidal sedimentation during a mid-Proterozoic marine transgression, Reynolds Range Group, Arunta Block, central Australia. Australian Journal of Earth Sciences 37, 409–422.

Dirks, P.H.G.M., Norman, A.R., 1992. Physical sedimentation processes on a mid-Proterozoic (1800 Ma) shelf: the Reynolds Range Group, Arunta Block, central Australia. Precambrian Research 59, 225–241.

Eriksson, K.A., Simpson, E.L., 1998. Controls on spatial and temporal distribution of Precambrian eolianites. Sedimentary Geology 120, 275–294.

Eriksson, P.G., Catuneanu, O., Nelson, D.R., Popa, M., 2005. Controls on Precambrian sea level change and sedimentary cyclicity. Sedimentary Geology 176, 43–65.

Evans, D.A.D., 2000. Stratigraphic, geochronological, and paleomagnetic constraints upon the Neoproterozoic climatic paradox. American Journal of Science 300, 347–433.

Evans, D.A., Beukes, N.J., Kirschvink, J.L., 1997. Low-latitude glaciation in the Palaeoproterozoic era. Nature 386, 262–266.

Fisher, R., 1953. Dispersion on a sphere. Proceedings of the Royal Society of London A217, 295–305.

Gellatly, D.C., Derrick, G.M., Plumb, K.A., 1970. Proterozoic palaeocurrent directions in the Kimberley region, northwestern Australia. Geological Magazine 107, 249–257.

Gellatly, D.C., Halligan, R., 1971. Charnley, Western Australia, 1:250,000 Geological Series Explanatory Notes, Sheet SE51-4. Bureau of Mineral Resources, Geology & Geophysics, Canberra, 35 pp. (http://www.ga.gov.au/map/#geology).

Gellatly, D.C., Derrick, G.M., Plumb, K.A., 1975. The geology of the Lansdowne 1:250,000 sheet area, Western Australia. Bureau of Mineral Resources, Geology & Geophysics, Canberra, Report 152, 100 pp.

Gray, H.H., 2001. Subglacial meltwater channels (Nye channels or N-channels) in sandstone at Hindostan Falls, Martin County, Indiana. Proceedings of the Indiana Academy of Science 110, 1–8.

Griffin, T.J., Grey, K., 1990. Kimberley Basin. In: Geology and Mineral Resources of Western Australia. Geological Survey of Western Australia Memoir 3, 293–304.

Griffin, T.J., Tyler, I.M., Playford, P.E., 1993. Lennard River, Western Australia, 1:250,000 Geological Series Explanatory Notes, Sheet SE51-8, 3rd edition. Geological Survey of Western Australia, Perth, 56 pp. (http://www.ga.gov.au/map/#geology).

Halilovic, J., Cawood, P.A., Jones, J.A., Pirajno, F., Nemchin, A.A., 2004. Provenance of the Earaheedy Basin: implications for assembly of the Western Australian Craton. Precambrian Research 128, 343–366.

Hendrickx, M., Slater, K., Crispe, A., Dean, A., Vandenberg, L., Smith, J., 2000. Palaeoproterozoic stratigraphy of the Tanami Region: regional correlations and relation to mineralisation—preliminary results. Northern Territory Geological Survey Record GS 2000–13, 28.

Hilburn, I.A., Kirschvink, J.L., Tajika, E., Tada, R., Hamano, Y., Yamamoto, S., 2005. A negative fold test on the Lorrain Formation of the Huronian Supergroup: uncertainty on the paleolatitude of the Paleoproterozoic Gowganda glaciation and implications for the great oxygenation event. Earth and Planetary Science Letters 232, 315–332.

Hoffman, P.F., Schrag, D.P., 2002. The snowball Earth hypothesis: testing the limits of global change. Terra Nova 14, 129–155.

Idnurm, M., 2000. Towards a high resolution Late Palaeoproterozoic—earliest Mesoproterozoic apparent polar wander path for northern Australia. Australian Journal of Earth Sciences 47, 405–429.

Idnurm, M., 2004. Precambrian palaeolatitudes for Australia—an update. Report prepared for Geoscience Australia, Canberra, 20 pp.

Idnurm, M., Giddings, J.W., 1988. Australian Precambrian polar wander. Precambrian Research 40–41, 61–88.

Idnurm, M., Senior, B.R., 1978. Palaeomagnetic ages of Late Cretaceous and Tertiary weathered profiles in the Eromanga Basin, Queensland. Palaeogeography, Palaeoclimatology. Palaeoecology 24, 263–277.

Idnurm, M., Giddings, J.W., Plumb, K.A., 1995. Apparent polar wander and reversal stratigraphy of the Palaeo–Mesoproterozoic southeastern McArthur Basin, Australia. Precambrian Research 72, 1–41.

Jenkins, G.S., McMenamin, M.A.S., McKay, C.P., Sohl, L. (Eds.), 2004. The Extreme Proterozoic: Geology, Geochemistry and Climate, American Geophysical Union Geophysical Monograph 146, 229 pp.

Kent, J.T., Briden, J.C., Mardia, K.V., 1983. Linear and planar structure in ordered multivariate data as applied to progressive demagnetization of palaeomagnetic remanence. Geophysical Journal of the Royal Astronomical Society 75, 593–621.

Kruse, P.D., Sweet, I.P., Stuart-Smith, P.G., Wygralak, A.S., Pieters, P.E., Crick, I.H., 1994. Katherine, Northern Territory, 1:250,000 Geological Series Explanatory Notes, Sheet SD53-9. Northern Territory Geological Survey, Darwin, 69 pp.

Li, Z.X., 2000. Palaeomagnetic evidence for unification of the North and West Australian cratons by *ca.* 1.7 Ga: new results from the Kimberley Basin of northwestern Australia. Geophysical Journal International 142, 173–180.

Li, Z.X., Powell, C.McA., Bowman, R., 1993. Timing and genesis of Hamersley iron-ore deposits. Exploration Geophysics 24, 631–636.

McElhinny, M., 2004. Geocentric axial dipole hypothesis: a least squares perspective. In: Channell, J.E.T., Kent, D.V., Lowrie, W., Meert, J.G. (Eds.), Timescales of the Paleomagnetic Field, American GeophysicalUnion Geophysical Monograph 145, pp. 1–12.

McElhinny, M.W., Evans, M.E., 1976. Palaeomagnetic results from the Hart Dolerite of the Kimberley Block, Australia. Precambrian Research 3, 231–241.

McFadden, P.L., 1990. A new fold test for palaeomagnetic studies. Geophysical Journal International 103, 163–169.

McNaughton, N.J., Rasmussen, B., Fletcher, I.R., 1999. SHRIMP uranium–lead dating of xenotime in siliciclastic sedimentary rocks. Science 285, 78–80.

Myers, J.S., Shaw, R.D., Tyler, I.M., 1996. Tectonic evolution of Proterozoic Australia. Tectonics 15, 1431–1446.

Ozchron, 2004. Ozchron National Geochronology database, Geoscience Australia, Canberra (http://www.ga.gov.au/oracle/ozchron/TOC.jsp).

Page, R., Sun, S.-S., 1994. Evolution of the Kimberley region, W.A. and adjacent Proterozoic inliers—new geochronological constraints. Geological Society of Australia Abstracts 37, 332–333.

Page, R.W., Griffin, T.J., Tyler, I.M., Sheppard, S., 2001. Geochronological constraints on tectonic models for Australian Palaeoproterozoic high-K granites. Journal of the Geological Society of London 158, 535–545.

Park, J.K., 1997. Paleomagnetic evidence for low-latitude glaciation during deposition of the Neoproterozoic Rapitan Group, Mackenzie Mountains, N.W.T., Canada. Canadian Journal of Earth Sciences 34, 34–49.
Pavlov, A.A., Hurtgen, M.T., Kasting, J.F., Arthur, M.A., 2003. Methane-rich Proterozoic atmosphere? Geology 31, 87–90.
Pesonen, L.J., Elming, S.-Å., Mertanen, S., Pisarevsky, S., D'Agrella-Filho, M.S., Meert, J.G., Schmidt, P.W., Abrahamsen, N., Bylund, G., 2003. Palaeomagnetic configuration of continents during the Proterozoic. Tectonophysics 375, 289–324.
Pirajno, F., Jones, J.A., Hocking, R.M., Halilovic, J., 2004. Geology and tectonic evolution of Palaeoproterozoic basins of the eastern Capricorn Orogen, Western Australia. Precambrian Research 128, 315–342.
Plumb, K.A., Gemuts, I., 1976. Precambrian geology of the Kimberley region, western Australia, 25th International Geological Congress, Sydney, Excursion Guide 44C, 69 pp.
Plumb, K.A., McGovern, J.L., 1968. Cambridge Gulf, W.A. Sheet SE 52-14. Bureau of Mineral Resources, Geology & Geophysics, and Geological Survey of Western Australia 1:250,000 Geological Series (http://www.ga.gov.au/map/#geology).
Plumb, K.A., Ahmad, M., Wygralak, A.S., 1990. Mid-Proterozoic basins of the north Australian Craton—regional geology and mineralisation. In: Hughes, F.E. (Ed.), Geology of the Mineral Deposits of Australia and Papua New Guinea, Volume 1, Australasian Institute of Mining & Metallurgy Monograph 14, pp. 881–902.
Roberts, H.G., Webb, W.W., McGovern, J.L., 1966. Mount Elizabeth, W.A. Sheet SE 52-1. Bureau of Mineral Resources, Geology & Geophysics, and Geological Survey of Western Australia 1:250,000 Geological Series (http://www.ga.gov.au/map/#geology).
Schmidt, P.W., 1993. Palaeomagnetic cleaning strategies. Physics of the Earth and Planetary Interiors 76, 169–178.
Schmidt, P.W., Clark, D.A., 1994. Palaeomagnetism and magnetic anisotropy of Proterozoic banded-iron formations and iron ores of the Hamersley Basin, Western Australia. Precambrian Research 69, 133–155.
Schmidt, P.W., Embleton, B.J.J., 1976. Palaeomagnetic results from sediments of the Perth Basin, Western Australia, and their bearing on the timing of regional lateritisation. Palaeogeography, Palaeoclimatology, Palaeoecology 19, 257–273.
Schmidt, P.W., Embleton, B.J.J., 1985. Prefolding and overprint magnetic signatures in Precambrian (~2.9–2.7 Ga) igneous rocks from the Pilbara Craton and Hamersley Basin, NW Australia. Journal of Geophysical Research 90, 2967–2984.
Schmidt, P.W., Williams, G.E., 1995. The Neoproterozoic climatic paradox: Equatorial palaeolatitude for Marinoan glaciation near sea level in South Australia. Earth and Planetary Science Letters 134, 107–124.
Schmidt, P.W., Williams, G.E., 1999. Paleomagnetism of the Paleoproterozoic hematitic breccia and paleosol at Ville-Marie, Québec: further evidence for the low paleolatitude of Huronian glaciation. Earth and Planetary Science Letters 172, 273–285.
Schmidt, P.W., Williams, G.E., 2002. Palaeomagnetic dating of the Hamersley Surface and deep weathering in the Pilbara—northern Yilgarn region. Geological Society of Australia Abstracts 67, 431.
Schmidt, P.W., Currey, D.T., Ollier, C.D., 1976. Sub-basaltic weathering, dam-sites and the age of laterisation. Journal of the Geological Society of Australia 23, 367–370.
Schmidt, P.W., Williams, G.E., Camacho, A., Lee, J.K.W., 2006. Assembly of Proterozoic Australia: implications of a revised pole for the ~1070 Ma Alcurra Dyke Swarm, central Australia. Geophysical Journal International 167, 626–634.
Shaw, R.D., Tyler, I.M., Griffin, T.J., Webb, A., 1992. New K–Ar constraints on the onset of subsidence in the Canning Basin, Western Australia. BMR Journal of Australian Geology and Geophysics 13, 31–35.
Sheppard, S., Tyler, I.M., Hoatson, D.M., 1997. Geology of the Mount Remarkable 1:100 000 Sheet, Explanatory Notes. Geological Survey of Western Australia, Perth, 27 pp.
Sheppard, S., Griffin, T.J., Tyler, I.M., Page, R.W., 2001. High- and low-K granites and adakites at a Palaeoproterozoic plate boundary in northwestern Australia. Journal of the Geological Society of London 158, 547–560.
Thorne, A.M., Sheppard, S., Tyler, I.M., 1999. Lissadell, Western Australia, 1:250,000 Geological Series Explanatory Notes, Sheet SE52-2, 2nd edition. Western Australia Geological Survey, Perth, 68 pp. (http://www.ga.gov.au/map/#geology).
Turner, P., 1980. Continental Red Beds. Elsevier, Amsterdam, 562 pp.
Tyler, I.M., Griffin, T.J., Shaw, R.D., 1991. Early Palaeozoic tectonism and reactivation of pre-existing basement structures at the margins of the Kimberley Craton, Western Australia. Geological Society of Australia Abstracts 31, 70–71.
Tyler, I.M., Sheppard, S., Bodorkos, S., Page, R.W., 2005. Tectonic significance of detrital zircon age profiles across Palaeoproterozoic orogens in the Kimberley region of northern Australia. Geological Society of Australia Abstracts 81, 33.
Williams, G.E., 1969. Stratigraphy and Sedimentation in the Mount Bedford Area, WA. Report to The Broken Hill Proprietary Company Limited, Melbourne.
Williams, G.E., Schmidt, P.W., 2004. Neoproterozoic glaciation: reconciling low paleolatitudes and the geologic record. In: Jenkins, G.S., McMenamin, M.A.S., McKay, C.P., Sohl, L. (Eds.), The Extreme Proterozoic: Geology, Geochemistry and Climate, American Geophysical Union Geophysical Monograph 146, pp. 145–977.
Williams, G.E., 2005. Subglacial meltwater channels and glaciofluvial deposits in the Kimberley Basin, Western Australia: 1.8 Ga low-latitude glaciation coeval with continental assembly. Journal of the Geological Society of London 162, 111–124.
Williams, G.E., 2008. Proterozoic (pre-Ediacaran) glaciation and the high obliquity, low-latitude ice, strong seasonality (HOLIST) hypothesis: principles and tests. Earth-Science Reviews 87, 61–93.
Williams, G.E., Schmidt, P.W., 1997. Paleomagnetism of the Paleoproterozoic Gowganda and Lorrain formations, Ontario: low paleolatitude for Huronian glaciation. Earth and Planetary Science Letters 153, 157–169.
Williams, G.E., Schmidt, P.W., 2004. Neoproterozoic glaciation: reconciling low paleolatitudes and the geologic record. In: Jenkins, G.S., McMenamin, M.A.S., McKay, C.P., Sohl, L. (Eds.), The Extreme Proterozoic: Geology, Geochemistry and Climate, American Geophysical Union Geophysical Monograph 146, pp. 145–159.
Williams, G.E., Schmidt, P.W., Clark, D.A., 2004. Palaeomagnetism of iron-formation from the late Palaeoproterozoic Frere Formation, Earaheedy Basin, Western Australia: palaeogeographic and tectonic implications. Precambrian Research 128, 367–383.
Wingate, M.T.D., Pirajno, F., Morris, P.A., 2004. The Warakurna large igneous province: a new Mesoproterozoic large igneous province in west-central Australia. Geology 32, 105–108.
Young, G.M., 2004. Earth's earliest extensive glaciations: tectonic setting and stratigraphic context of Paleoproterozoic glaciogenic deposits. In: Jenkins, G.S., McMenamin, M.A.S., McKay, C.P., Sohl, L. (Eds.), The Extreme Proterozoic: Geol-ogy, Geochemistry and Climate, American Geophysical Union Geophysical Monograph 146, pp. 161–181.
Young, G.M., Long, D.G.F., Fedo, C.M., Nesbitt, H.W., 2001. Paleoproterozoic Huronian basin: product of a Wilson cycle punctuated by glaciations and a meteorite impact. Sedimentary Geology 141–142, 233–254.
Zhao, G., Cawood, P.A., Wilde, S.A., Sun, M., 2002. Review of global 2.1–1.8 Ga orogens: implications for a pre-Rodinia supercontinent. Earth-Science Reviews 59, 125–162.
Zhao, G., Sun, M., Wilde, S.A., Li, S., 2004. A Paleo–Mesoproterozoic supercontinent: assembly, growth and breakup. Earth-Science Reviews 67, 91–123.